Microscopic model for the magnetic-field-driven breakdown of the dissipationless state in the integer and fractional quantum Hall effect

A. Poux,[1] Z. R. Wasilewski,[2,3,4] K. J. Friedland,[5] R. Hey,[5] K. H. Ploog,[5] R. Airey,[6] P. Plochocka,[1] and D. K. Maude[1,*]

[1]*Laboratoire National des Champs Magnétiques Intenses, CNRS-UGA-UPS-INSA, 143 avenue de Rangueil, 31400 Toulouse, France*

[2]*Institute for Microstructural Sciences, National Research Council, Ottawa, Canada*

[3]*Department of Electrical and Computer Engineering, University of Waterloo, Canada*

[4]*Department of Physics and Astronomy, Waterloo Institute for Nanotechnology, Waterloo, Canada*

[5]*Paul Drude Institut für Festkörperelektronik, Berlin, Germany*

[6]*Department of Electronic and Electrical Engineering, University of Sheffield, United Kingdom*

(Received 1 June 2016; published 9 August 2016)

Intra-Landau-level thermal activation, from localized states in the tail to delocalized states above the mobility edge in the same Landau level, explains the $B_c(T)$ (half width of the dissipationless state) phase diagram for a number of different quantum Hall samples with widely ranging carrier density, mobility, and disorder. Good agreement is achieved over two to three orders of magnitude in temperature and magnetic field for a wide range of filling factors. The Landau-level width is found to be independent of magnetic field. The mobility edge moves in the case of changing Landau-level overlap to maintain a sample dependent critical density of states at that energy. An analysis of filling factor $\nu = 2/3$ shows that the composite fermion Landau levels have exactly the same width as their electron counterparts. An important ingredient of the model is the Lorentzian broadening with long tails which provide localized states deep in the gap which are essential in order to reproduce the robust high-temperature $B_c(T)$ phase observed in experiment.

DOI: 10.1103/PhysRevB.94.075411

I. INTRODUCTION

The integer quantum Hall effect [1,2] (QHE) can in principle be understood within the framework of a single-particle picture. The quantized plateaux in the Hall resistance R_{xy} together with the zero resistance state in the longitudinal resistance R_{xx} occur whenever the Fermi energy lies in a gap in the density of states. When a two-dimensional electron gas (2DEG) is placed in a perpendicular magnetic field, the movement of the Fermi energy through the quantized Landau levels is driven by the eB/h degeneracy of a spin Landau level. For a two-dimensional carrier density n_s, the filling factor is defined as $\nu = n_s h/eB$. At even filling factors E_f lies in a cyclotron gap while for odd filling factors it lies in a spin gap. This picture only gives rise to quantum Hall states of nonzero width in the presence of disorder broadened Landau levels, with localized states in the tails, beyond a sharp mobility edge. As we move away from an exact integer filling factor, the dissipationless resistance is quenched once the increasing (decreasing) eB/h degeneracy drives the Fermi energy into the delocalized states near the Landau-level center.

Thus, understanding the nature of the disorder is important if we are to fully understand the quantum Hall effect, with important implications for metrology. Disorder acts subtly; it simultaneously strengthens the integer QHE (wider plateau, larger critical current), while competing with or even annihilating the fractional QHE. For example, the competition between the disorder induced energy cost of reversing spins, and the exchange energy gain, controls the opening of the many-body spin gap at odd filling factors [3,4]. Indeed, the shape of the disorder broadened, Landau levels remains controversial. In an exquisitely difficult experiment, a detailed analysis of the sawtooth form of the extremely small oscillations in the 2DEG magnetization versus magnetic field, essentially the weight of the higher harmonic terms in a Liftshitz-Kosevich approach, suggested that the Landau-level broadening is Lorentzian [5]. However, subsequent work led to diverging conclusions [6,7]. The presence of disorder is also naturally required to explain the fractional QHE [8–12] within the composite fermion framework, in which the fractional filling factors for electrons map to integer filling factors on noninteracting composite fermions, quantized into Landau levels by an effective quantizing magnetic field $B^* = B - B_{1/2}$ [13].

It has been shown that the width in magnetic field (ΔB) of the maxima in R_{xx}, the so-called plateau to plateau transitions in R_{xy}, follows a universal scaling law with $\Delta B \propto T^{\kappa}$ where $\kappa = 0.42$ is universal [14,15]. The scaling law was derived using renormalization group theory (RGT), which is generally applied to problems (phase transitions) which are too complicated to solve from first principles. The universality is the expected signature of a quantum phase transition [16]. However, the experimental universal value of $\kappa = 0.42$ turned out to be controversial, with some later work establishing a universal value of $\kappa = 0.58$ which was tentatively attributed to a non-Fermi-liquid-like behavior [17–30].

In a different approach, Rigal and co-workers reported that the phase diagram for the (half) width of the dissipationless state, in the longitudinal resistance R_{xx}, versus magnetic field of a quantum Hall sample bears a remarkable resemblance to the phase diagram for the critical magnetic field of a high-temperature superconductor with vortex melting [31]. This can be seen in Fig. 1 where we replot the $B_c(T)$ phase diagram with the data taken from Ref. [31]. As discussed by Rigal *et al.*, all even integer filling factors show a low-temperature Gorter-Casimir-like phase with, perhaps surprisingly, the same (extrapolated) critical temperature $T_c^{LT} \simeq 1.5$ K. In the high-temperature phase the critical temperature T_c^{HT} for even

*duncan.maude@lncmi.cnrs.fr

 ©2016 American Physical Society

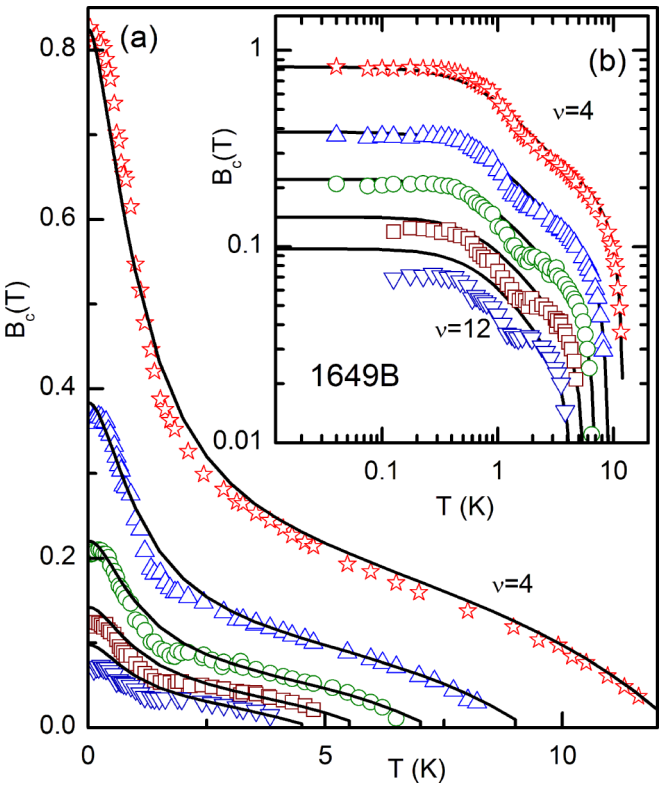

FIG. 1. (a) Critical magnetic field (half width of the dissipationless region) versus temperature for integer quantum Hall filling factors $\nu = 4,6,8,10,12$ for sample 1649B. The data are taken from Ref. [31]. The solid curves are the calculated critical magnetic field due to thermal activation of carriers to delocalized states above the mobility edge in the disorder broadened Landau level. (b) A log-log plot of the same data and calculations.

filling factors scales approximately as the cyclotron gap. The low-temperature values of the critical magnetic field scale as $B_c(\nu) = B_{c0}(1/\nu^2 - 1/\nu_0^2)$ consistent with Landau levels with a constant (filling factor independent) ratio of the number of localized to delocalized states within a Landau level. Here ν_0 is the filling factor above which the conduction is no longer dissipationless at $T = 0$ K. The $1/\nu^2$ scaling arises from the Landau-level degeneracy $eB_f/h\nu$ (magnetic field $B = B_f/\nu$ where B_f is the magnetic field at which $\nu = 1$ occurs), and the fact that for every magnetic flux quanta added (or removed), ν electrons disappear (or appear) in the Landau level at the Fermi energy (since there are ν occupied Landau levels below or at E_f which gain or lose an electron).

In this paper, we show that the $B_c(T)$ phase diagram of Rigal *et al.* can be exactly explained by a simple model involving thermal activation from localized states in the tails, to the delocalized state near the center, of a disorder broadened Landau level at the Fermi energy. This work is then extended, to a number of different 2DEG samples with very different carrier densities and mobilities, for both even, odd, and fractional filling factors. Our results strongly suggest that Landau-level broadening is Lorentzian. The long Lorentzian tails are a fundamental requirement to explain the robust high-temperature $B_c(T)$ phase. In other words, it is essential to have a significant number of states, deep in the gap, into which the Fermi level can be pushed in order to suppress thermal activation at the high critical temperatures observed in experiment. We will see that Gaussian broadening simply fails to meet this stringent requirement.

We stress that the Lorentzian line shape is found for all the samples investigated, including a high mobility–low disorder 2DEG which shows well developed fractional quantum Hall states. The model can equally well explain the $B_c(T)$ phase diagram for even, odd and fractional filling factors, with a self-consistent limited parameters set, for each sample, explaining the data at all filling factors. From the data set and model, a global and coherent picture emerges, in which the mobility edge, normally assumed to be fixed, can move under conditions of changing Landau-level overlap. This occurs for example, in the case of (i) the emergence of a single-particle spin gap in the Landau level at the Fermi energy for even filling factors, (ii) the emergence of a many body spin gap at odd filling factors, and (iii) in the case of the overlap of localized states in the tails of Landau levels at low magnetic fields. This can all be understood within the framework of conduction via variable range hopping [32–38] in the Landau-level tails. Overlapping the *localized* states of different Landau levels increases the density of states at the Fermi energy, increasing the probability of variable range hopping, i.e., causes the mobility edge to shift further away from the center of the Landau level. Thus, what is required to have a robust quantum Hall sample is large disorder, in order to have a large Landau-level broadening, with an even larger gap to avoid at all cost the overlap of the localized tails. This probably goes a long way to explain the current interest in graphene for metrology [39–41].

The rest of the paper is arranged as follows: In Sec. II the intra-Landau-level thermal activation model using Fermi-Dirac statistics is presented and demonstrated to work well for the previously published $B_c(T)$ phase diagram in Ref. [31]. This result is then extended to other samples. In Sec. III a brief description of the experimental techniques and sample characteristics are presented. Results, for three very different 2DEG samples, are presented in Sec. IV. The thermal activation model is shown to work for even, odd, and fractional filling factors in widely different samples. For certain samples, in which the Landau-level overlap is changing, a clear signature of the movement of the mobility edge is observed. In Sec. V the implications of this work for scaling theory are discussed. Finally, global conclusions are drawn and the implications and outlook for future work are drawn in Sec. VI.

II. INTRA-LANDAU-LEVEL THERMAL ACTIVATION TO THE MOBILITY EDGE

We propose a simple microscopic model, based on thermal activation *within* the partially occupied Landau level at the Fermi energy, which can explain both the low- and high-temperature phases in the B_c versus T phase diagram for *all filling factors*. A Lorentzian broadening of the Landau level is used, with the assumption that states in the tails are localized and do not contribute to transport, while states in the center, above a sharp mobility edge, are delocalized. For a given integer filling factor, at the critical temperature the Fermi level lies in the center of the gap and the zero resistance state is destroyed due to a thermally activated

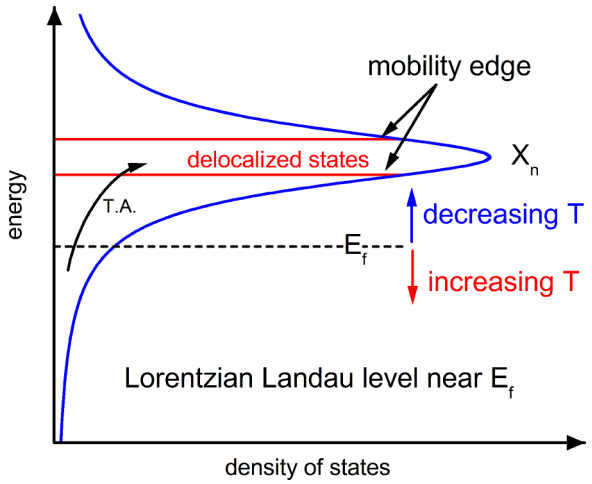

FIG. 2. Schematic showing intra-Landau-level thermal activation with a Lorentzian broadening. As sketched the single-particle Zeeman energy is much smaller than the broadening so that spin splitting can be neglected. The required movement of E_f with temperature, in order to maintain the dissipationless state, is indicated by the vertical arrows. In the experiment the Fermi energy is moved by changing the magnetic field (filling factor).

(critical) population ν_c of delocalized states just above the mobility edge. This explains why the high-temperature phase has a critical temperature $T_c^{HT}(\nu)$ which scales approximately with the cyclotron gap for even filling factors. With decreasing temperature, it is possible to push the Fermi energy up, closer to the mobility edge, before the critical occupation ν_c is obtained (see Fig. 2). At $T = 0$, to a good approximation, the Fermi energy coincides with the mobility edge. Thus, the low-temperature value of B_c is simply controlled by the fraction of delocalized states in the Landau level. An important ingredient of this model is the line shape used to describe the disorder broadening of the Landau level. The robustness of the B_c versus T phase diagram in Ref. [31] results from the Lorentzian Landau-level broadening, with its extremely long tails which provide a wide range of possible Fermi energies, and hence a wide range of temperature over which the dissipationless regime is maintained. Other line shapes (e.g., Gaussian) have short tails and are unable to reproduce the robust high-temperature phase. An important part of this work is extending this result to a range of samples with very different mobilities and disorder.

The spin Landau levels are described using two Lorentzians,

$$g_{n\uparrow\downarrow}(E) = \frac{1}{\pi\Gamma\left[1+\left(\frac{E-X_{n\uparrow\downarrow}}{\Gamma}\right)^2\right]},$$

where

$$X_{n\uparrow\downarrow} = \left(n+\frac{1}{2}\right)\hbar\omega_c \pm \frac{1}{2}g^*\mu_B B.$$

Each Lorentzian is centered at $X_{n\uparrow\downarrow}$ with a full width at half maximum of 2Γ. The Lorentzians, as written, are normalized so that the integral over all energies $\int g_{n\uparrow\downarrow}(E)dE = 1$ and all calculations are performed using filling factor rather than carrier density.

For a given position of the Fermi energy E_f, the filling factor can be obtained using

$$\nu(T,E_f) = \int_{-\infty}^{\infty}\sum_{n=0}^{\infty}[g_{n\uparrow}(E)+g_{n\downarrow}(E)]f(E)dE, \quad (1)$$

where $f(E) = 1/\{1+\exp[(E-E_f)/KT]\}$ is the Fermi-Dirac distribution function. The integral is computed numerically and to speed up the calculation we consider only Landau levels in the direct vicinity of the Fermi energy (i.e., the Landau levels immediately above and below E_f). Other Landau levels are assumed to be either full or empty. Knowing the filling factor we can calculate the magnetic field which corresponds to the current position of the Fermi energy, $B = B_f/\nu$ where $B_f = n_s h/e$ is the magnetic field at which filling factor $\nu = 1$ occurs in a sample with carrier density n_s.

In this simple model, the dissipationless resistance state ceases to exist when the thermally activated population of delocalized states above the mobility edge exceeds a critical value [which depends on the value of the critical resistance R_c used to determine the half width (B_c) of the dissipationless state]. At low temperatures, this thermal activation occurs from electrons occupying states below the mobility edge in the *same Landau level*. This explains why the low-temperature phase has the same critical temperature ($T_c^{LT} \simeq 1.5$ K) for all filling factors, i.e., it does not depend on the size of the cyclotron gap. With increasing temperature, the Fermi energy is pushed further and further down into the tail of the Landau level, in order to maintain the occupation of the delocalized states below the critical value. Thus, the width in temperature of the low-temperature phase is very sensitive to the size (Γ) of the Landau-level broadening. At $T = 0$, the resistance lifts off, when the mobility edge coincides with the Fermi energy, so that $B_c(T = 0)$ depends only on the number of localized states below the mobility edge, i.e., Γ/Γ_{dl}.

Thermal broadening is included phenomenologically by writing

$$\Gamma(T) = \sqrt{\Gamma(0)^2+(\alpha KT)^2},$$
$$\Gamma_{dl}(T) = \Gamma_{dl}(0)\sqrt{1+[\alpha KT/\Gamma(0)]^2},$$

where $\alpha \sim 1$ is a dimensionless parameter. Note that the ratio Γ_{dl}/Γ is independent of the temperature.

For a given even integer filling factor ($\nu = 2n$), temperature and position of E_f, the population of delocalized states above the mobility edge in the Landau level directly above the Fermi energy is given by

$$\delta\nu(T,E_f) = \int_{X_{n\uparrow}-\Gamma_{dl}}^{X_{n\uparrow}+\Gamma_{dl}} g_{n\uparrow}(E)f(E)dE + \int_{X_{n\downarrow}-\Gamma_{dl}}^{X_{n\downarrow}+\Gamma_{dl}} g_{n\downarrow}(E)f(E)dE. \quad (2)$$

The critical temperature in the high-temperature phase, which scales as the cyclotron energy, corresponds to the situation where E_f lies exactly at midgap and the resistance starts to lift off due to thermal activation across the gap. While the critical population of delocalized states could be taken as a fitting parameter, it makes more sense to use experiment to fix this value; for each filling factor we use the observed

critical temperature of the high-temperature phase, to calculate the (critical) population, $\delta\nu_c$, of delocalized state above the mobility edge, when E_f lies in the center of the cyclotron gap.

Assuming that the obtained value of $\delta\nu_c$, for a given filling factor, does not depend on the temperature, we calculate iteratively for each temperature the required position of E_f using Eq. (2) to have the critical occupation $\delta\nu_c$ of the delocalized states. A valid solution is found if E_f lies somewhere between midgap and the center of the Landau level. Then, using the value of E_f we calculate using Eq. (1) the filling factor and hence the magnetic field. We calculate the cyclotron energy $\hbar\omega_c = \hbar eB/m^*$ and the Zeeman energy $g\mu_B B$ using the magnetic field $B = B_f/\nu$ corresponding to the even integer filling factor. Within this approximation, the problem is symmetric with respect to moving away from integer filling factor to lower or higher fields, i.e., the partial filling factor ε (when $\delta\nu = \delta\nu_c$) of electrons in the previously empty, of holes in the previously full Landau level is the same. In other words the filling factors found are $\nu + \varepsilon$ and $\nu - \varepsilon$ corresponding to magnetic fields $B_1 = B_f/(\nu + \varepsilon)$ and $B_2 = B_f/(\nu - \varepsilon)$ with $B_c = (B_2 - B_1)/2$. A second iteration, using this time the previous values of B_1 and B_2 to calculate the cyclotron and Zeeman energies only changes B_c by a few mT and was thus judged to be unnecessary. The approximation works well because (i) B_1 and B_2 are generally not too different from B_f/ν (ν is an even integer) and (ii) the corrections to B_1 and B_2 actually tend to cancel. The cyclotron energy is calculated using the accepted effective mass in GaAs, corrected for nonparabolicity in the higher density samples [42]. To calculate the Zeeman energy we use the accepted value of the Landé g factor in bulk GaAs $g^* = -0.44$ which is different from 2 due to spin-orbit coupling [43].

In the model we have three fitting parameters: (i) the Landau-level broadening Γ which is adjusted to have the correct width of the low-temperature phase, (ii) the position of the mobility edge (number of localized states) which is controlled by Γ_{dl}, essentially the ratio Γ_{dl}/Γ determines the value of $B_c(T \to 0)$, and (iii) the thermal broadening parameter α which improves the agreement at high temperatures. The experimental value of T_c^{HT} used to define $\delta\nu_c$ ensures that $B_c \to 0$ at the correct temperature. The solid lines in Fig. 1 are calculated using $\Gamma = 3.0$ K, $\Gamma_{dl} = 0.9\Gamma$, $\alpha = 1$, $m^* = 0.072m_e$, and $g^* = -0.44$. As can be seen in the log-log plot in Fig. 1(b), this single parameter set provides a good fit to all even filling factors, over nearly three orders of magnitude in temperature and almost two orders of magnitude in magnetic field.

Similar calculations using a Gaussian line shape reveal the importance of the long Lorentzian tails for the robustness of the high-temperature part of the $B_c(T)$ phase diagram. As an example in Fig. 3(a) we show calculations for a Lorentzian broadening performed with the same conditions and parameter set as for $\nu = 4$ for sample 1649B (which fit the data perfectly). For calculations using the Gaussian broadened Landau level, the width of the Landau level is precisely determined by the width of the low-temperature part of the $B_c(T)$ phase diagram where B_c is rapidly falling, and the width of the delocalized states (position of the mobility edge Γ_{dl}) is determined by the value of $B_c(T \to 0)$. For $T > 1$ K the predicted values of B_c are significantly lower than required and for $T > 4$ K the predicted B_c falls below the experimental limit at which we can measure, i.e., the high-temperature phase is predicted to be washed out. The short Gaussian tails do not have sufficient states with energies well below the mobility edge in order that B_c survives up to the temperature at which activation across the cyclotron gap finally kills the dissipationless state. The Gaussian and Lorentzian Landau levels are sketched in Fig. 3(b) with the broadening used in the calculations. The position of the mobility edge is indicated by the vertical broken lines. Note that the parameters given for the Landau-level broadening (Γ) is half of the full width at half maximum (FWHM).

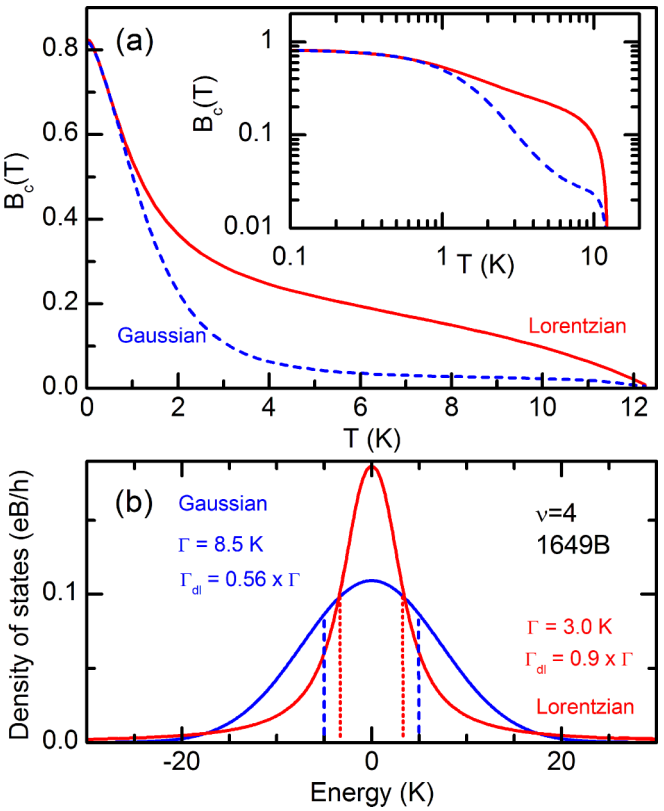

FIG. 3. (a) Calculated $B_c(T)$ for Lorentzian and Gaussian broadened Landau levels. For the Lorentzian we have used the parameters and conditions of $\nu = 4$ in sample 1649B. The width of the Gaussian is precisely determined by the width of the $B_c(T)$ for $T < 1$ K and completely fails to reproduce the data for $T > 1$ K. The inset shows a log-log plot of the same curves. (b) The Lorentzian and Gaussian Landau levels drawn according to the parameters used in the fits. Vertical broken lines indicate the approximate position of the mobility edge. Note spin splitting is not resolved for either line shape.

For the moment we have focused uniquely on the simplest case of even integer filling factors; when the Fermi energy lies in the cyclotron gap, the system is spin unpolarized, so that the spin gap is given by the single-particle Zeeman energy $g^*\mu_B B$ and many-body effects can safely be neglected. However, it is trivial to extend the thermal activation model to odd filling factors, where the Fermi energy lies in the spin gap. This gap can be reproduced using an effective g factor $g^*_{\text{eff}} \gg g^*$ due to the many-body enhancement of the spin gap in the spirit of the Ando model [44]. Equally, the model can be

extended to fractional states, within the composite fermion framework [13]. A crucial test of the thermal activation model will be its ability to explain the $B_c(T)$ phase diagram for even, odd, and fractional filling factors in different samples with widely different characteristics. Such an investigation will be presented in the the following sections.

III. EXPERIMENTAL TECHNIQUES

For the electrical transport measurements the sample was placed in the mixing chamber of a top loading dilution refrigerator equipped with a 16-T superconducting magnet. The sample and wires are immersed directly in the He^3/He^4 mixture. During the top loading, the sample is cooled slowly over a number of hours. In contrast to previous measurements all data were taken during the same cool down in the dilution refrigerator. Temperatures in the range 10 mK–4.2 K were obtained with the sample in liquid. For higher temperatures up to $\simeq$12 K the mixture was removed with the exception of a few mbars of exchange gas. The temperature was controlled either using a heater mounted directly in the mixing chamber a few cm from the sample, and/or by controlling the amount of He exchange gas in the inner vacuum chamber of the refrigerator. This was achieved via the temperature of a sorb pump (small piece of activated charcoal) placed in the vacuum chamber.

Hall bars were fabricated using standard photolithography techniques with an aspect ratio of 3:1, e.g., a Hall bar width of 250 μm with 750 μm between the voltage contacts. A constant low current of 10–20 nA at 10.66 Hz was applied using a 100-MΩ series resistor and the oscillator output of an SR830 lockin amplifier. Low-pass preamplifiers, based on the INA111 Burr Brown low noise operational amplifier, were placed as close to the sample probe as feasible to keep cable lengths below 50 cm for the unamplified signal. The longitudinal resistance R_{xx} was measured using phase sensitive detection. The sample temperature was monitored using RuO_2 ($T <$ 4.2 K) and Cernox ($T >$ 4.2 K) thermometers placed close to the sample. The thermometers were also measured using preamplifiers and phase-sensitive detection using 1 nA (RuO_2) and 10 nA (Cernox) current at 18.15 Hz.

The R_{xx} versus magnetic field (0–16 T) were measured with a sweep speed of 0.25 T/min, slow enough to avoid (i) heating the refrigerator and (ii) shifting the high-field quantum Hall data due to the 300-ms time constant of the lock-in amplifier. For the Dingle plots, particulary for the high mobility–high-density samples, very slow sweeps were performed (0.005–0.05 T/min) to avoid damping the amplitude of the fast oscillations. We also corrected the data for the −27-mT remnant magnetic field of our superconducting coil which was determined from the characteristic zero-field weak localization cusp in R_{xx}. The critical magnetic field was determined, as in Ref. [31], by defining an arbitrary critical resistance $R_c = 10\ \Omega$, chosen to be above the noise level in our system. For a current of 20 nA this corresponds to a voltage of 200 nV across the voltage contacts of the sample.

All the GaAs/AlGaAs 2DEGs investigated were grown by molecular beam epitaxy using solid sources and modulation doping. Sample 1649A is another piece of the same wafer as sample 1649B used in Ref. [31]. It has an 8.2-nm-wide GaAs quantum well. Sample 1707 is a standard high mobility GaAs/AlGaAs heterojunction. Sample 1200 is a 13-nm-wide GaAs quantum well sandwiched between short period GaAs/AlAs superlattices which act as the barriers. The two short period superlattices each have 60 periods of 4 monolayers (MLs) of AlAs and 8 MLs of GaAs. Carriers are introduced into the central 13-nm GaAs quantum well by a single Si δ-doping sheet with a concentration of 2.5×10^{12} cm^2 placed in a GaAs layer of each short period superlattice. Carriers also occupy donor states associated with the X conduction-band minimum in the AlAs superlattice barriers. At low temperatures they are frozen out and do not contribute to transport. However, they are very efficient at screening the potential fluctuations due to the δ doping giving unusually large mobilities for a high density 2DEG [45,46]. The Landau-level broadening was determined from a Dingle analysis of the low-field data at mK temperatures. The Dingle plots of $\Delta R_{xx}/R_{xx}(0)$ versus $1/B$ are shown in Fig. 4. All samples show a linear behavior over one to two orders of magnitude in resistance. The solid lines are the linear fits used to estimate the Landau-level broadening. A summary of all sample parameters can be found in Table I. The mobilities have been calculated from the measured $T = 0$ resistivity and the carrier density using $\mu = 1/n_s e\rho$. To estimate the ratio τ_t/τ_q of the transport and the single-particle (quantum) lifetime we have used $\mu = e\tau_t/m^*$ and $\tau_q = \hbar/2\Gamma_D$. Values of τ_t/τ_q of 20 are typical for high mobility 2DEGs due to the reduced influence [factor of $1 - \cos(\theta)$] of the small-angle scattering

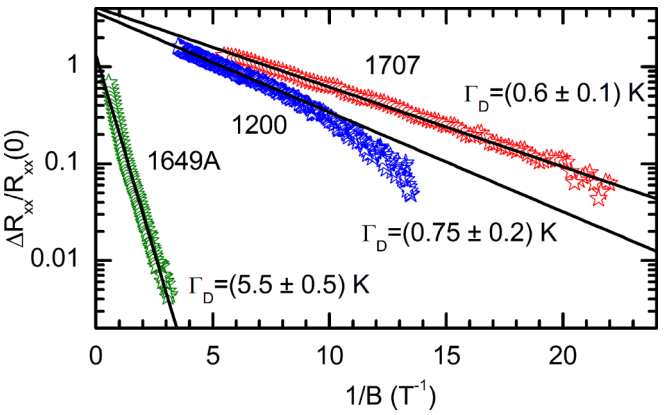

FIG. 4. Dingle plot of the amplitude of the oscillation $\Delta R_{xx}/R_{xx}(0)$ vs inverse magnetic field for the three samples investigated. The solid lines are linear fits used to extract the Landau-level broadening.

TABLE I. Summary of the sample parameters; the carrier density n_s, the transport mobility $\mu = e\tau_t/m^*$, the Landau-level broadening determined from the Dingle plot $\Gamma_D = \hbar/2\tau_q$, and the ratio of the transport and quantum lifetimes τ_t/τ_q. Note the FWHM of the Landau levels is $2\Gamma_D$.

Sample	n_s (cm^{-2})	μ (cm^2/V s)	Γ_D (K)	τ_t/τ_q
1649B	7.28×10^{11}	1.0×10^5		
1649A	7.28×10^{11}	7.5×10^4	5.5	5
1707	1.54×10^{11}	4.1×10^6	0.6	25
1200	7.49×10^{11}	2.5×10^6	0.75	20

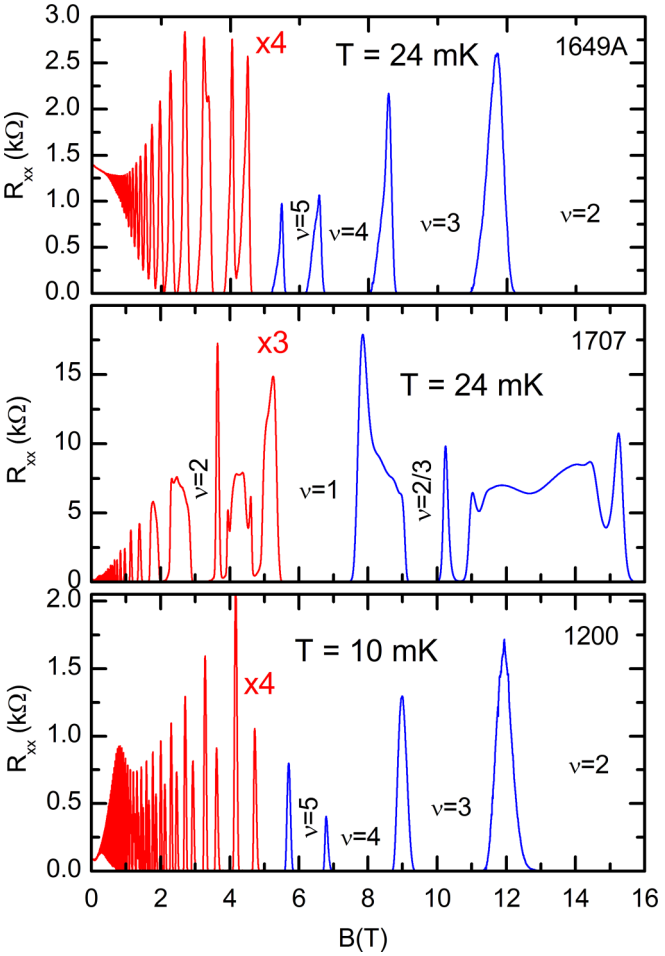

FIG. 5. The longitudinal resistance R_{xx} as a function of magnetic field at low temperature for the three samples investigated. The resistance in the low-field regions has been multiplied by the indicated factors to make the data at high filling factors more visible.

on the transport lifetime. This is reduced to a factor of roughly 5 for the low mobility quantum well sample 1649.

IV. EXPERIMENTAL RESULTS AND DISCUSSION

Figure 5 shows the low-temperature R_{xx} versus magnetic-field traces between 0 and 16-T for the three samples investigated. All samples show well defined integer quantum Hall states. Their properties are summarized in Table I.

Sample 1649A is a low mobility–high-density 2DEG with broad Landau levels with a high proportion of localized states in the tails. It displays wide regions of dissipationless conduction in the vicinity of integer filling factors. Sample 1707 is a low-density–high mobility 2DEG with narrow Landau levels and few localized states in the Landau-level tails. It displays relatively narrow regions of dissipationless conduction in the vicinity of integer filling factors. 1707 is a typical fractional quantum Hall sample which shows the standard series of fractions around filling factor $\nu = 1/2$ and $\nu = 3/2$, notably a well developed $\nu = 2/3$ state with a wide region of dissipationless conductance. Sample 1200 shows a very similar high-field $R_{xx}(B)$ trace as sample 1649 due to the similar densities and proportion of localized states.

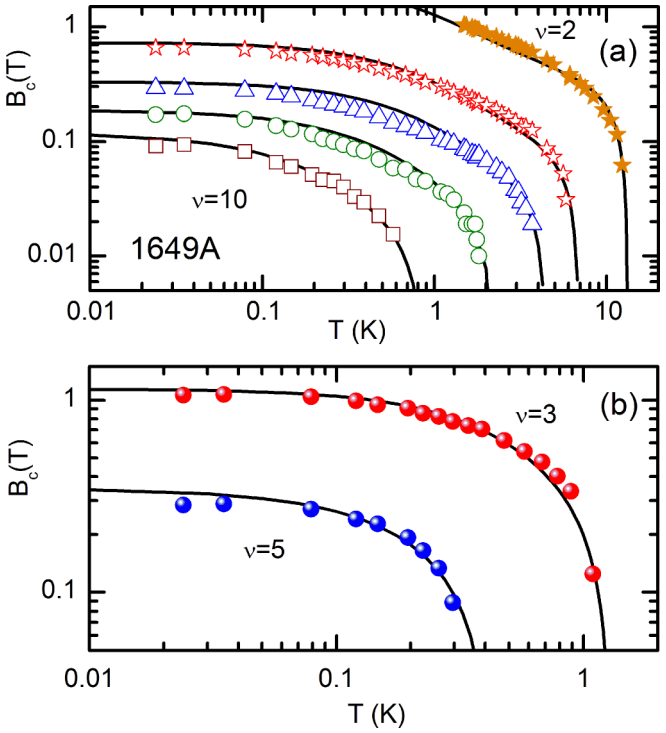

FIG. 6. Critical magnetic field vs temperature plotted as log-log for sample 1649A for (a) various even filling factors and (b) various odd filling factors. The solid lines are calculated using the thermal activation model as described in the text.

In order to determine the $B_c(T)$ phase diagram we have made an extremely detailed temperature dependence of $R_{xx}(B)$ for each sample. Below we present the results sample by sample together with the fits to the thermal activation model. Global conclusions, comparing the behavior of the three samples in order to probe the validity of the assumptions made in the thermal activation model, will be drawn in the discussion section. We will see that a self-consistent picture emerges, with clear evidence that the mobility edge actually moves if spin splitting at even filling factors is suppressed, or if the Landau-level broadening or overlap changes.

A. Sample 1649A—high density–large disorder–low mobility

Samples 1649A is another piece of the same wafer as 1649B [$B_c(T)$ data presented in Fig. 1]. We have completely repeated the measurements to have a full data set for both odd and even filling factors and to have an estimate of the Landau-level width from a Dingle analysis (see Sec. III). In this sample we have access to even filling factors $\nu = 2,4,6,8,10$, although the high-field extremity of $\nu = 2$ is only in field range for high temperatures ($T > 1$ K). We have well developed dissipationless regions for odd filling factors $\nu = 3,5$, with inevitably filling factor $\nu = 1$ out of the available field range. The $B_c(T)$ phase diagram is plotted in Fig. 6 for both odd and even filling factors. For even filling factors the phase diagram is quasi-identical to that measured previously for 1649B, although the values of B_c found are slightly lower.

Fitting to the lowest even integer filling factor for which we have data over the full temperature range ($\nu = 4$), we obtain

TABLE II. Summary of the parameters used in the thermal activation model; the effective mass m^* in GaAs corrected for nonparabolicity in the high density samples, the factor α used to include thermal broadening, the $T = 0$ width of the Landau levels Γ, the ratio of the width of the localized and delocalized states Γ_{dl}/Γ for even, odd, and fractional filling factors, the Landé g factor g^* for GaAs, and the effective g factor $g^*_{\rm eff}$ to describe the exchange enhanced spin gap at odd filling factors, and for fractional filling factors the composite Fermi effective mass and g factor.

	All				Even		Odd		Fractional		
Sample	B_f (T)	$m^*(m_e)$	α	Γ (K)	Γ_{dl}/Γ	g^*	Γ_{dl}/Γ	$\lvert g^*_{\rm eff}\rvert$	Γ_{dl}/Γ	$m^*_{cf}(m_e)$	g^*_{cf}
1649B	30.15	0.072	1.0 ± 0.1	3.0 ± 0.3	0.9 ± 0.1	−0.44					
1649A	30.15	0.072	1.0 ± 0.1	3.4 ± 0.3	1.1 ± 0.1	−0.44	0.3 ± 0.05	2.4			
1707	6.37	0.067	0.3 ± 0.05	0.23 ± 0.05	1.5 ± 0.1	−0.44	1.5 ± 0.1	2.5–7.5	0.9 ± 0.1	0.8 ± 0.1	−0.44
1200	31.00	0.072	1.25 ± 0.1	0.9 ± 0.1	1.3−0.58	−0.44	0.58 ± 0.05	5.0–7.0			

$\Gamma = 3.4$ K, similar to the value found for 1649B, but slightly smaller than the broadening, determined from the Dingle analysis, of $\Gamma_D = 5.5$ K suggesting a narrowing of the Landau levels at high field. The value of $B_c(T \to 0)$ fixes $\Gamma_{dl} = 1.1\Gamma$, slightly larger than the value found for 1649B (0.9Γ) indicating that 1649A has fewer localized states which leads to the slightly lower values of B_c. An excellent fit to the $\nu = 4$ data is obtained using the same thermal broadening parameter $\alpha = 1$ [solid line in Fig. 6(a)]. The cyclotron gap was calculated using an effective mass $m^* = 0.072m_e$ slightly larger than the band-edge mass in GaAs due to nonparabolicity [42]. The thermal activation model is then used to calculate the $B_c(T)$ phase diagram for all the even integer filling factors with *no adjustable parameters*. The agreement with experiment is remarkable confirming our simple model in which the Landau-level width is independent of magnetic field, with a mobility edge which does not move (i.e., Γ_{dl}/Γ is constant, independent of the filling factor).

For odd filling factors we fit to the $\nu = 3$ data, fixing all parameters as for the even filling factors (see Table II), with the exception of $\Gamma_{dl} = 0.3\Gamma$ and an effective g factor for the many-body enhanced spin gap $g^*_{\rm eff} = 2.4$. The fit is again excellent [solid lines Fig. 6(b)] for both $\nu = 3$ and 5. This demonstrates that as for the even filling factors the Landau-level broadening and the position of the mobility edge is independent of the filling factor. Γ_{dl} is approximately a factor of 4 smaller than for the even integer case demonstrating that the opening of the spin gap causes the mobility edge to shift significantly towards the center of the Landau level creating many more localized states in the tail of the Landau level. On the other hand Γ is unchanged for odd and even filling factors showing that the opening of the spin gap does not affect the Landau-level broadening.

B. Sample 1707—low density–low disorder–large mobility

In sample 1707 we have access to even filling factor $\nu = 2,4,6,8$ and odd filling factors $\nu = 1,5,7$. For some reason in this sample the $\nu = 3$ minimum in R_{xx} has an asymmetric shape, lifting off prematurely on the high-field side and never actually falls below the $R_c = 10\Omega$ cut-off used to determine B_c. In addition, 1707 has several prominent fractions, of which only $\nu = 2/3$ is fully developed, with R_{xx} falling below the $R_c = 10\Omega$ cutoff. Unfortunately, $\nu = 1/3$ remains out of our field range, even at higher temperatures. The $B_c(T)$ phase diagram is plotted in Fig. 7 for both odd, even, and fractional filling factors. Compared to 1649, the even integer filling factors have relatively small values of B_c at low temperature reflecting the lower magnetic field at which they occur (due to the lower carrier density) and the greatly reduced disorder in this sample.

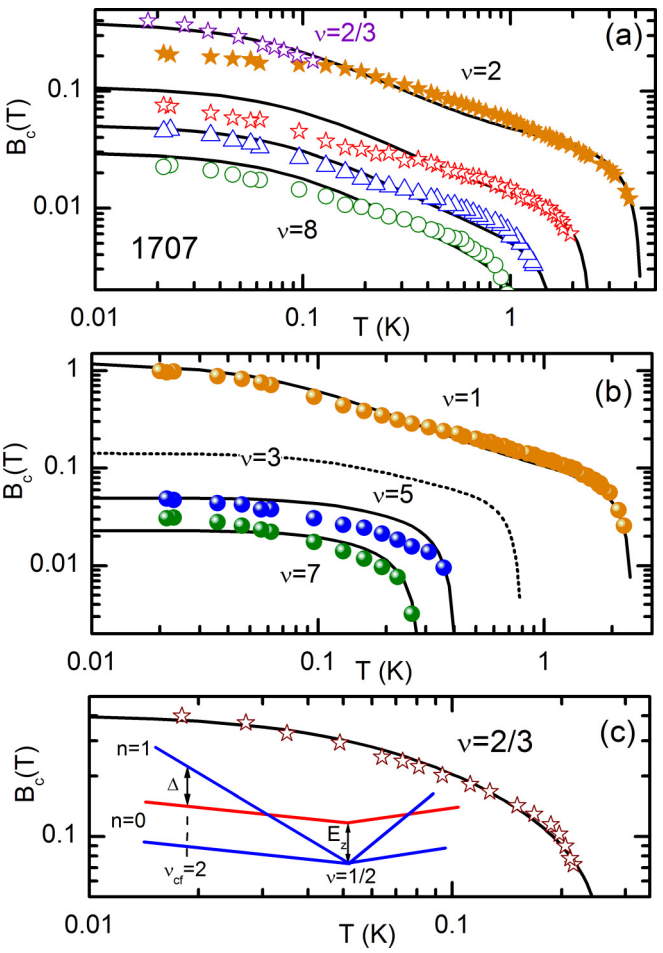

FIG. 7. Critical magnetic field vs temperature plotted as log-log for sample 1707 for (a) various even, (b) odd, and (c) fractional filling factors. The solid lines are calculated using the thermal activation model as described in the text. The inset shows a schematic of the composite fermion Landau levels around $\nu = 1/2$. In (a) we plot also the data of $\nu = 2/3$ which is the composite fermion filling factor $\nu_{cf} = 2$. The agreement with electron filling factor $\nu = 2$ data is remarkable.

While we could adopt the same procedure as for sample 1649, fitting to $\nu = 2$ to obtain the correct parameters, and then generating curves for all the other filling factors without any adjustable parameters, it turns out that this is not the best approach. There is a suspicion that the even filling factors are fragile in this sample, and the low-temperature values of B_c may be lower than they should be for whatever reason, e.g., despite the small current used the Hall electric field may shift the mobility edge. In addition, the parameters obtained by fitting to the $\nu = 2$ data do not fit extremely well the other filling factors; notably the predicted low-temperature values of B_c are *lower* than the measured values.

Fitting to the $\nu = 1$ data, we obtain a Landau-level broadening $\Gamma = 0.23$ K, lower than the value obtained from a Dingle analysis $\Gamma_D = 0.6$ K suggesting again that the Landau-level width at high field is considerably reduced compared to the low-field value. We stress that the width of the low-temperature phase of the $B_c(T)$ phase diagram is very sensitive to the width of the Landau level so that Γ is determined quite precisely. The experimental value of $B_c(T \to 0)$ is correctly reproduced with $\Gamma_{dl} = 1.5\Gamma$ which is much larger than the value (0.3Γ) obtained for odd filling factors in 1649A; the fraction of localized states is much lower in sample 1707. Thermal broadening effects are also very small with $\alpha = 0.3$. As for 1649 the agreement between the predictions of the thermal activation model and the $\nu = 1$ data is excellent over nearly two orders of magnitude in temperature and magnetic field. Using the same parameter set, reasonable agreement is obtained for filling factors $\nu = 5$ and 7. The size of the many-body spin gap has been calculated using a filling factor dependent effective g factor $g^*_{\rm eff} = 2.5$–7.5 to correctly reproduce the observed temperature dependence of $B_c(T)$.

The predicted $B_c(T)$ for even filling factors is then calculated using exactly the same parameter set as for the odd filling factors (see Table II). In this low-density sample, the cyclotron gap was calculated using an effective mass $m^* = 0.067$ which is the band-edge mass in GaAs. The agreement between model (solid lines) and the data is good with some deviation at low temperatures with the measured values being too low, especially for $\nu = 2$. As for sample 1649A, odd and even filling factors can be fitted with the same Landau-level broadening Γ. However, in stark contrast, both sets of filling factors can be fitted without moving the mobility edge, e.g., the same value of Γ_{dl}/Γ. This would be consistent with the small single-particle spin gap being open, in the absence of exchange interactions, at spin unpolarized even filling factors. This is reasonable since in 1707, the single-particle Zeeman energy $E_z \simeq 1$ K (at $\nu = 2$) is much greater than the Landau-level width $\Gamma = 0.23$ K.

The idea that the experimental values of $B_c(T)$ are too low at low temperatures is comforted by the data for $\nu = 2/3$ which corresponds to composite fermion filling factor $\nu_{cf} = 2$ [13]. In this picture, the many-body fractional quantum Hall effect of electrons is mapped to the integer quantum Hall effect of non-interacting composite fermion quasiparticles. Composite fermions are formed by attaching two fictitious magnetic-flux quantum, antiparallel to the applied magnetic field, to each electron. In a mean-field picture, composite fermions move in an effective magnetic field $B^* = B - B_{1/2}$ where $B_{1/2}$ is the magnetic field at electron filling factor $\nu = 1/2$. The low-temperature $\nu = 2/3$ data, plotted in Fig. 7(a), lie above the $\nu = 2$ data, indicating that the composite fermion $\nu_{cf} = 2$ state is more robust than its electron counterpart, and is in excellent agreement with the prediction of the activation model for electron filling factor $\nu = 2$.

Finally, we apply the activation model to the $\nu = 2/3$ fractional state [see Fig. 7(c)]. In the framework of the composite fermion model we treat this state as an effective $\nu_{cf} = 2$ state. We can fit to the data with $\Gamma = 0.23$ confirming a previous report, based on a Dingle analysis, that the composite fermions and electrons have identical Landau-level broadening [47]. The value of $B_c(T \to 0)$ fixes $\Gamma_{dl} = 0.9\Gamma$. Imposing $g^* = -0.44$ for the noninteracting composite fermions an excellent fit is obtained with $m^*_{cf} = 0.8m_e$. Leadley *et al.* reported that the composite fermion mass varies as a function of the effective magnetic field B^* [47]. In our sample $\nu = 2/3$ occurs at $B^* \simeq 3.2$ T (the same magnetic field as $\nu = 2$). The literature value for composite fermion mass at B^* is $m^*_{cf} \simeq (0.7$–$1.0)m_e$, in reasonable agreement with our value [47,48]. For electrons, in the activation model the effective mass essentially controls the gap at even filling factors (corrections due to the single-particle Zeeman energy are negligible). For composite fermions the situation is complicated by the large mass, which reduces the cyclotron gap, and by the effectively larger single-particle Zeeman energy, which depends on the total magnetic field $(3B_f/2)$ rather than $B^* = B_f/2$. For our parameter set we have at $\nu_{cf} = 2$, a cyclotron energy $\hbar\omega_c \simeq 5.4$ K and a Zeeman energy $E_z = 2.9$ K. As $\hbar\omega_c > E_z$ this implies that the ground state is spin unpolarized (the spin up and down $n = 0$ composite fermion spin Landau levels are occupied) and excitations involve a spin flip to the $n = 1$ composite fermion Landau level. The situation with the composite fermion Landau levels is shown schematically in the inset of Fig. 7(c). The energy gap for the excitation is $\Delta = \hbar\omega_c - E_z$, which depends on both the effective mass and the composite fermion g factor.

C. Sample 1200—high density–large disorder–high mobility

Sample 1200 is a rather unusual 2DEG due essentially to the superlattice barriers. It has a high carrier density together with a high mobility, but also a rather large disorder in the sense that it has narrow Landau levels but a large proportion of localized states. This combination gives rise to a large number of accessible odd ($\nu = 3$–11) and even ($\nu = 4$–12) filling factors. Here we have limited the analysis of even filling factors to states which have $B_c(T \to 0) > 50$ mT. The $B_c(T)$ phase diagram is plotted in Fig. 8 for odd and even filling factors. Both show robust dissipationless states with values of B_c at low temperatures comparable to the highly disordered sample 1649.

As for sample 1707, we start by fitting to the lowest odd filling factor $\nu = 3$. The width of the low-temperature phase is best described with a Landau-level broadening of $\Gamma = 0.9$ K, which in contrast to the other samples is actually larger than the broadening $\Gamma_D = 0.75$ K extracted from a Dingle analysis of the low-field oscillations. The value of $B_c(T \to 0)$ fixes the position of the mobility edge with $\Gamma_{dl} = 0.58\Gamma$. We use a cyclotron mass $m^* = 0.072m_e$ to correct for nonparabolicity, a thermal broadening parameter $\alpha = 1.25$, and the many-body enhanced spin gap is calculated using an effective g

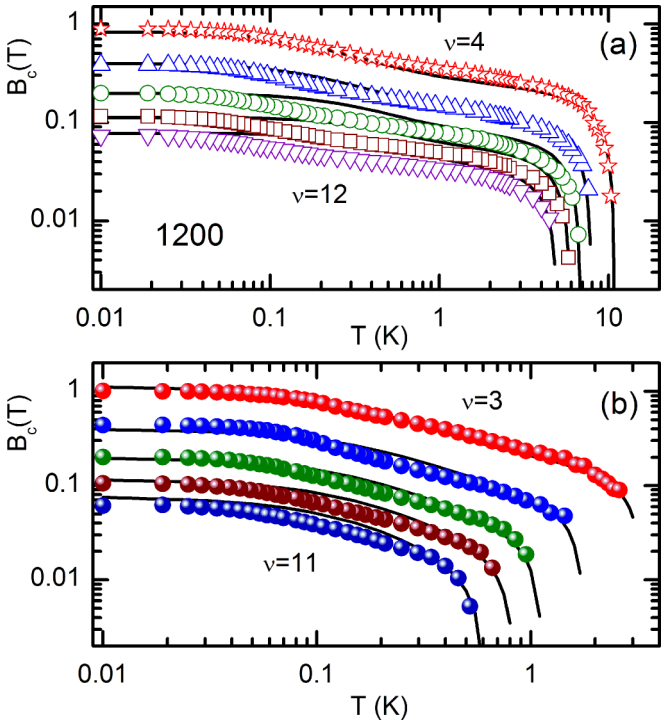

FIG. 8. Critical magnetic field vs temperature plotted as log-log for sample 1200 for (a) various even filling factors and (b) various odd filling factors. The solid lines are calculated using the thermal activation model as described in the text.

factor $g^*_{\rm eff} = 7.0$. The agreement between the model (solid line) and experiment is excellent. The curves for the other filling factors can then be generated with $g^*_{\rm eff} = 7.0$–5.0 as the only adjustable parameter. As for the other samples the data for all filling factors is well reproduced over two to three orders of magnitude in magnetic field and temperature. This demonstrates that for the odd filling factors the Landau level broadening and the position of the mobility edge are independent of filling factor. Note that this conclusion, which can be drawn from the $B_c(T \to 0)$ data alone, is independent of the value of $g^*_{\rm eff}$ used, which simply improves the fit at intermediate temperatures.

To fit the even filling factors we start with an identical parameter set as for the odd filling factors, with of course the exception that the spin gap is calculated with the single-particle g factor $g^* = -0.44$. An excellent fit is obtained for $\nu = 4$ and $\nu = 6$. For lower filling factors the $B_c(T \to 0)$ data can only be reproduced by assuming that the mobility edge is shifting outwards into the tail of the Landau level. With this assumption, reasonable fits are obtained using $\Gamma_{dl} = 0.58$, 0.58, 0.9, 1.24, and 1.3Γ for filling factors $\nu = 4$, 6, 8, 10, 12 respectively. The agreement is not as good as for the other samples; while the values of $B_c(T \to 0)$ are perfectly reproduced, the predicted values of B_c at intermediate temperatures is too large indicating that the Landau-level broadening decreases at filling factors above $\nu = 6$. This discrepancy is also visible for the higher odd filling factors. The decrease of Γ in this sample, possibly linked to the changing ratio of the magnetic length and the characteristic length scale of the disorder potential, would necessarily cause the mobility edge to shift outwards, as required to fit to the $B_c(T \to 0)$ data.

If the single-particle spin gap was open at $\nu = 4$ and $\nu = 6$ before progressively closing for higher filling factors this would also cause the mobility edge to shift out. This is plausible as the single-particle Zeeman energy $E_z \simeq 1.2$ K at $\nu = 8$ is comparable to the Landau-level broadening $\Gamma = 0.9$ K. However, if the Landau-level broadening is decreased then the spin gap should remain open for the higher filling factors.

D. Discussion—Validity and limits of the model

The picture which emerges from fitting the $B_c(T)$ phase diagram for odd and even filling factors for the three samples above can be summarized as follows. The Landau-level broadening and the position of the mobility edge within the Landau level are independent of the magnetic field (Landau-level index) provided the overlap of the spin-up and spin-down sublevels is not changing. Under such conditions the simple intra-Landau-level thermal activation model provides an accurate description of the $B_c(T)$ phase diagram for all filling factors with a single parameter set. As the single-particle Zeeman energy is small, paradoxically odd filling factors, with their large exchange enhanced spin gaps, fulfill this condition for all of the investigated samples. The behavior at even filling factors, for which there is no enhanced spin gap, depends on the size of the single-particle Zeeman energy compared to the Landau-level broadening. In sample 1707 with it extremely narrow Landau levels, to a first approximation the spin gap remains fully open at even integer filling factors, and both odd and even filling factors can be fitted with the same position of the mobility edge. In sample 1649, the Landau levels are broad and the spin gap remains closed at even filling factors. Two different positions of the mobility edge are required for even and odd filling factors. Finally, in sample 1200, while the odd filling factors are well behaved and can be fitted with a single position for the mobility edge, for even filling factors, the spin gap is opening at lower filling factors and the mobility edge shifts closer to the Landau level center, finally reaching the same value as for odd filling factors.

At the critical magnetic field, breakdown occurs due to the onset of variable range hopping in the tail of the Landau level. At $T = 0$, the mobility edge corresponds to the critical density of states at the Fermi level. In analogy to the quasielastic inter-Landau-level scattering (QUILLS) model [49], in this case in the absence of electric field and within the same Landau level, we can estimate the number of states in the Landau level which have sufficient wave function overlap for tunneling. To have sufficient overlap, the states have to lie with a circle of radius $2A_n$, where $A_n = (2n+1)^{1/2}\ell_B$ is the classical turning point of the simple harmonic oscillator, $\ell_B = (h/eB)^{1/2}$ is the magnetic length, and n is the orbital quantum number. The Landau-level degeneracy can be written as $2\pi/\ell_B^2$ so that the number of states which can participate at an energy E (measured from the center of the Landau level) is given by

$$n_p(E) = \lambda \frac{8\pi^2(2n+1)}{\pi\Gamma(1+E^2/\Gamma^2)},$$

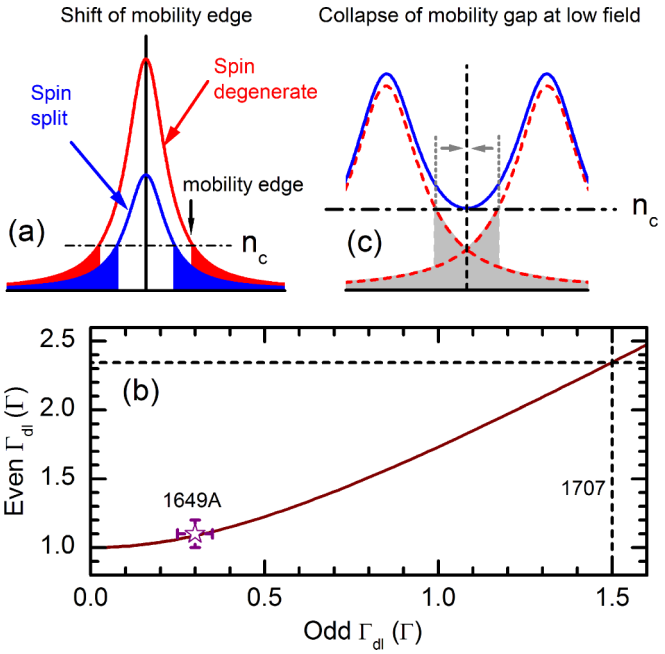

FIG. 9. (a) Schematic of the density of states of a Landau level with and without spin splitting. To maintain the same density of states, the mobility edge has to move towards the center of the Landau level when the spin degeneracy is lifted. (b) The solid line shows the predicted position of the model edge when the spin gap is closed versus the position of the mobility edge when the spin gap is open. The symbols shows the experimental values for sample 1649A. (c) Schematic showing two Landau levels (broken lines) strongly overlapping at low magnetic field. The solid line shows the total density of states while the grey areas show localized states (mobility edge) for nonoverlapping Landau levels. To maintain the same density of states (without overlap) the mobility edge has to shift towards the tail of the Landau level, eventually causing the mobility gap to collapse.

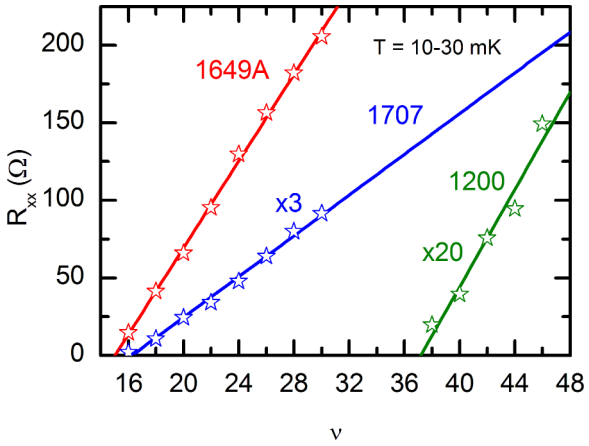

FIG. 10. Value of the low-temperature resistance vs even filling factor for the three samples investigated. The solid lines are linear fits. The intercept with the horizontal axis can be used to estimate the filling factor ν_0 at which the dissipationless state disappears at $T = 0$.

where $\lambda = 1$ if the Landau level is spin split or $\lambda = 2$ if the spin gap is closed. The magnetic lengths in the Landau-level degeneracy and A_n cancel leaving only the prefactor $(2n + 1)$ which describes the increased delocalization of the higher energy simple harmonic oscillator wave functions. Thus, in contrast with the experimental observation that the mobility edge remains fixed, the number of states close enough to tunnel is predicted to depend on the Landau-level index (magnetic field). In this picture, the mobility edge Γ_{dl} corresponds to the hopping threshold, when the critical number of states per unit area *at the same energy* $[n_c = n_p(\Gamma_{dl})]$ which can tunnel is achieved.

When the single-particle spin gap closes, $\lambda \to 2$ and the mobility edge will have to move to a new position further out (Γ'_{dl}) into the tail of the Lorentzian to maintain the critical density [see schematic in Fig. 9(a)]. The relation between the two values can be written as

$$\Gamma'_{dl} = \sqrt{\Gamma^2 + 2\Gamma_{dl}^2}.$$

In Fig. 9(b) we plot (solid line) the predicted position of the mobility edge Γ'_{dl} when the spin gap is closed versus Γ_{dl}. The measured value for sample 1649A (symbol) is in good agreement with the simple model. We cannot compare for the other samples since either the spin gap remains open (1707) or the mobility edge is moving continuously (1200).

Note also that comparing the values of Γ_{dl}/Γ (see Table II) for even filling factors gives the misleading impression that all samples have a similar disorder. This is due to the spin gap remaining open at even filling factors in sample 1707. Comparing Γ_{dl}/Γ for odd filling factors show that the width of the delocalized states is three to five times larger for sample 1707. The dashed lines in Fig. 9(b) indicates the expected value, for sample 1707, of $\Gamma_{dl}/\Gamma \simeq 2.35$ if the spin gap was closed at even filling factors.

Finally, it is interesting to consider the predictions of the activation model in the low-field limit for even filling factors. In Fig. 10 the resistance at even filling factors at low temperatures $(T \to 0)$ is plotted as a function of filling factor. The dependence is approximately linear and the intercept with the horizontal axis can be used to estimate the filling factor at which the conductance ceases to be dissipationless, $\nu_0 = 14$, 16, and 38 for samples 1649A, 1707, and 1200 respectively. Assuming that Γ_{dl}/Γ is independent of filling factor, we would naively expect that at $T = 0$ the dissipationless conductance would disappear at filling factor ν_0 when $2\Gamma_{dl} = E_c^{\nu=1}/\nu_0$ where $E_c^{\nu=1} = \hbar eB_f/m^*$ is the cyclotron energy at $\nu = 1$. This prediction is clearly wrong; for example for sample 1649A, using the parameters from Table II gives $\nu_0 \simeq 74$ while the conductance is no longer dissipationless for $\nu \geqslant 14$. What is not included in the model is the movement of the mobility edge as the adjacent Landau levels start to overlap; the mobility edge has to shift out so that the overlapping density of states at the mobility edge maintains the same value of n_c. The mobility gap finally collapses, when the combined density of states at the center of the cyclotron gap equals n_c [see Fig. 9(c)]. The condition for this can be written

$$\nu_0 = \frac{E_c^{\nu=1}}{2\sqrt{\Gamma^2 + 2\Gamma_{dl}^2}}. \quad (3)$$

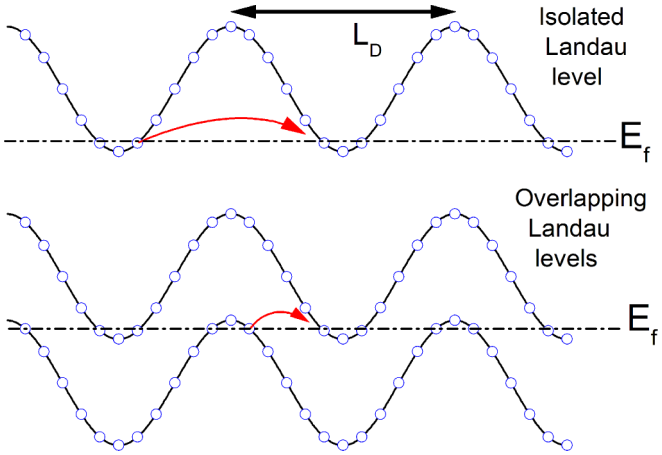

FIG. 11. Schematic of the spatial, disorder induced, potential fluctuations in a Landau level. The potential fluctuations have a characteristic length scale ℓ_D which controls the hopping distance required to find another state at the same energy (i.e., at the Fermi energy E_f). If the Landau levels overlap this distance is roughly halved.

This gives $\nu_0 \simeq 58$ for sample 1649A which is still too large. However, the above expression considers only states from the Landau levels immediately above and below the Fermi level which is not a good approximation. Taking into account contributions from all Landau levels the condition can be written as

$$\frac{2}{\pi\Gamma\left(1+\Gamma_{dl}^2/\Gamma^2\right)} = \sum_{n=0}^{\infty} \frac{2}{\pi\Gamma\left[1+\left(\frac{E_c^{\nu=1}}{2\nu_0\Gamma}\right)^2(\nu_0-1-2n)^2\right]}.$$

The left-hand side is the density of states (in units of eB/h) at the mobility edge of an isolated Landau level and the right-hand side is the sum of the density of states in the middle of the cyclotron gap (at the Fermi energy) for filling factor ν_0. If only the (identical) terms with $n = \nu_0/2$ and $n = -1 + \nu_0/2$ are retained, the expression can be rearranged to obtain the simplified expression of Eq. (3). The infinite sum converges rapidly and for our purposes it is more than enough to take into account the first 200 Landau levels. Using the parameters from Table II, the predicted values are $\nu_0 \simeq 38$ (1649A), $\nu_0 \simeq 68$ (1707), and $\nu_0 \simeq 132$ (1200) which are all significantly larger than the experimental values. This suggests that the overlap of multiple Landau levels causes the mobility edge to move out more rapidly than predicted by our simple model. All Landau levels see the same potential fluctuations, so that within a Landau level the minimum hop distance is given by the characteristic length of the disorder potential ℓ_D. The overlap between the high-energy tail of one Landau level, with the low-energy tail of another, will halve the minimum hopping distance to $\ell_D/2$ [see Fig. 11]. This is not included in the simple model; the reduced hopping distance will reduce the critical density of states required for hopping and cause the mobility edge to move rapidly outwards, precipitating the collapse of the mobility gap at low fields.

V. IMPLICATIONS FOR SCALING THEORY

In the pioneering work of Pruisken, a scaling theory of the plateau plateau (PP) or plateau insulator (PI) transitions in the QHE regime was developed, using renormalization-group theory (RGT), to describe the problem of a quantum phase transition which is too complicated to be solved from first principles [15]. The theory predicts a universal behavior, characteristic of a quantum phase transition, in which the width of the peak in R_{xx} scales as $\Delta B \propto T^{\kappa}$ where κ is universal. The theory predicts no particular value for κ and experiment from a log-log plot of $1/\Delta B$ versus T, and initially concluded that $\kappa = 0.42$ [14]. Subsequent work, including measurements on the same sample used in Ref. [14], found a larger value of $\kappa = 0.58$ [26–30]. In the original experiment, Wei *et al.* defined the peak width $\Delta B \propto T^{\kappa}$, whereas later work defined the width in terms of filling factor $\Delta\nu \propto T^{\kappa}$. As the filling factor is inversely proportional to the magnetic field the temperature dependence of ΔB and $\Delta\nu$ can be somewhat different; it is not obvious that if one follows a power law, the other will also follow the same power law [27].

Looking at the $B_c(T)$ data for all the samples investigated, it is clear that the lower filling factors have large regions, often over almost an order of magnitude in magnetic field and temperature, in which the dependence is linear. This suggests that $B_c(T)$ has a power-law dependence. We note that where the linear behavior persists to higher filling factors (see, e.g., inset of Fig. 1), the slope is always the same. In other words it appears to be quite universal in the sense it is independent of Landau-level index. In order to compare the $B_c(T)$ data, we plot in Fig. 12(a), using a double log scale, $B_c(T)$ for the lowest odd and even filling factor which show a linear dependence for the different samples investigated. All the plotted filling factors, both odd and even, have a linear region with identical slopes, suggesting that the power-law dependence is universal, independent of both the Landau-level index and the sample. The solid lines are the predicted power-law dependence $B_c \propto T^{\kappa}$ with $\kappa = 0.58$. Clearly, the agreement is remarkable given the identical slope observed for different filling factors from different samples. There is one exception: while $\nu = 3$ in sample 1200 has a large linear region with a slope close to $\kappa = 0.58$, the even filling factors (e.g., $\nu = 4$ which is not plotted in Fig. 12 for clarity), have a smaller slope $\simeq 0.29$. As our simple intra-Landau-level activation model correctly reproduces the data for a number of different samples with very different carrier densities and disorder, the question arises as to where the apparent universality comes from and what are the implications for the scaling theory which applies to the width of the maxima in R_{xx}?

In order to answer this question, we must first establish a link between ΔB (width of R_{xx} peak) of scaling theory and B_c (half width of R_{xx} minimum). In the intra-Landau-level activation model the problem is symmetric in filling factor (see Sec. II); when moving away from integer filling factor ν, the resistance ceases to be dissipationless at filling factors $\nu \pm \varepsilon$, corresponding to magnetic fields $B_1 = B_f/(\nu + \varepsilon)$ and $B_2 = B_f/(\nu - \varepsilon)$ with $B_c = (B_2 - B_1)/2$. Thus, we can write

$$B_c = \frac{B_f \varepsilon}{\nu^2(1-\varepsilon^2/\nu^2)},$$

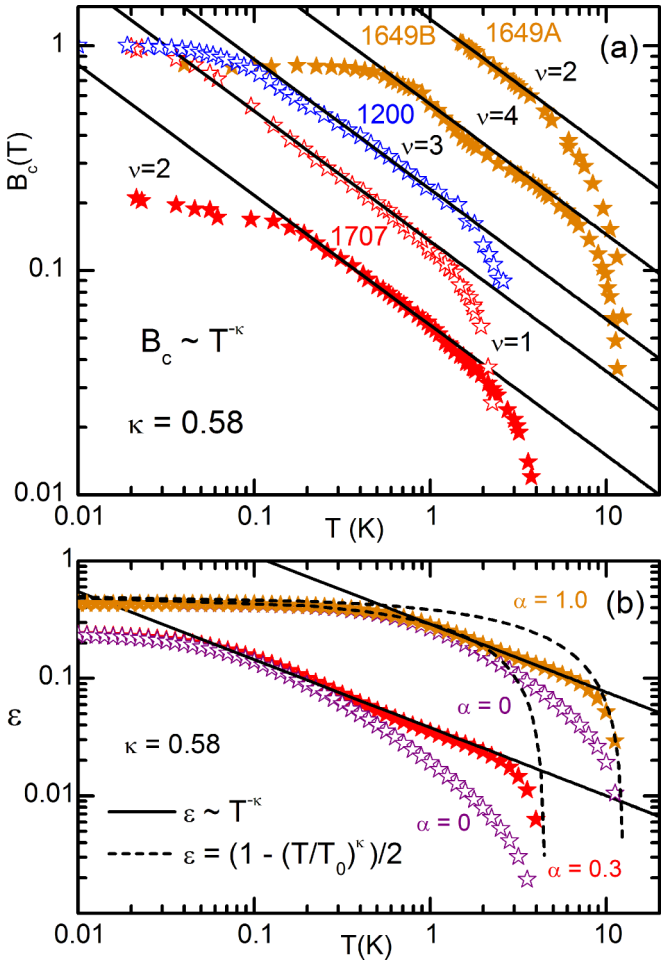

FIG. 12. (a) Log-log plot of $B_c(T)$ vs temperature for selected odd and even filling factors, which show a distinct linear regime, for all samples investigated. The solid lines show a power-law dependence with $B_c \propto T^{-\kappa}$ with $\kappa = 0.58$. (b) Log-log plot of the partial filling factor ε vs temperature calculated with the thermal activation model. The parameters used correspond to $\nu = 2$ in sample 1707 and $\nu = 4$ in sample 1649B (see Table II). The calculations are made with (closed symbols) and without (open symbols) thermal broadening. The solid lines are a power-law behavior $\varepsilon \propto T^{-\kappa}$ with $\kappa = 0.58$. The broken lines are the expected $\varepsilon(T) = [1 - (T/T_0)^{\kappa}]/2$ from scaling theory as described in the text.

which varies to a good approximation as $1/\nu^2$ (in agreement with experiment) with a small correction $(1 - \varepsilon^2/\nu^2)^{-1} \approx 1$ which deviates appreciably from 1 only for the lowest filling factor. Thus, $B_c \simeq B_f \varepsilon/\nu^2$. If we reason in terms of the filling factor, there is no approximation involved with a width of 2ε. The temperature dependence of B_c then arises from the temperature dependence of the partial filling factor $\varepsilon(T)$. If $B_c(T)$ scales as $T^{-\kappa}$ this implies that $\varepsilon \propto T^{-\kappa}$ [here we neglect $(1 - \varepsilon^2/\nu^2)^{-1} \approx 1$].

In a similar way the peak in R_{xx} between integer filling factors ν and $\nu - 1$ has a width $\Delta B = B_f/(\nu + \varepsilon - 1) - B_f/(\nu - \varepsilon)$. This can be rearranged to give

$$\Delta B = \frac{B_f(1 - 2\varepsilon)}{\nu^2 - \nu - \varepsilon(1 - \varepsilon)},$$

which provided $\nu^2 \gg \varepsilon(1 - \varepsilon)$ leads to $\Delta B \propto (1 - 2\varepsilon)$. Again, in terms of filling factor, there is no approximation involved, with a width of $1 - 2\varepsilon$. If ΔB is to scale as T^{κ} this implies that (within the framework of the activation model) $(1 - 2\varepsilon) = (T/T_0)^{\kappa}$. Thus, it is mathematically impossible that both $B_c(T)$ and $\Delta B(T)$ simultaneously have a power-law dependence; the observation of a scaling behavior for B_c precludes the observation of a scaling behavior for ΔB and vice versa.

In Fig. 12(b) we plot the temperature dependence of ε calculated using the thermal activation model with parameters corresponding to $\nu = 2$ in sample 1707 and $\nu = 4$ in sample 1649B. The calculations have been made with and without thermal broadening. The solid lines indicate a power-law dependence $\varepsilon \propto T^{-\kappa}$ with $\kappa = 0.58$. Without thermal broadening (open symbols), the slope of $\varepsilon(T)$ (on a log-log plot) changes continuously from horizontal at low T, to vertical at high T. With such a behavior it is inevitable that, at some point, the slope equals -0.58, at least over a limited temperature range. Including thermal broadening in the calculations (closed symbols) prolongs this behavior to higher temperatures, creating a wider range of temperatures over which $\varepsilon \propto T^{-\kappa}$ with $\kappa = 0.58$. Thus, we conclude that universality is explicitly absent from the intra-Landau-level thermal activation model (the slope changes continuously as a function of temperature), and the observed power-law behavior is generated by a sample (but not filling factor) dependent thermal broadening parameter. A power-law dependence of ΔB would require $(1 - 2\varepsilon) = (T/T_0)^{\kappa}$ which can be rearranged to give $\varepsilon = [1 - (T/T_0)^{\kappa}]/2$. The broken lines in Fig. 12(b) show the required behavior of ε. Scaling theory implicitly assumes that all states are localized at $T = 0$ ($\varepsilon = 0.5$), which is not what is found experimentally. However, the functional form is roughly correct; flat at low temperature and falling off rapidly at high temperature. Note that here, the T_0 parameter of scaling theory plays the role of the critical temperature at which the dissipationless conductance ceases to exist.

VI. CONCLUSION

A simple model involving thermal activation, from localized states in the tail of the Landau level at the Fermi energy, to delocalized states above the mobility edge in the same Landau level, explains the $B_c(T)$ phase diagram for a number of different quantum Hall samples with widely ranging carrier density, mobility, and disorder. Good agreement is achieved over two to three orders of magnitude in temperature and magnetic field for a wide range of filling factors. The width of the low-temperature $B_c(T)$ region depends sensitively on the Landau-level broadening Γ. For a given sample, both even and odd filling factors can be fitted with the same value of Γ demonstrating that the Landau-level width is independent of magnetic field in the high-field regime. The position of the mobility edge is also independent of magnetic field, provided the Landau-level overlap does not change. Our data suggest that the mobility edge moves to maintain a sample dependent critical density of states at that energy, leading to a simple relation between the position of the mobility edge with and without the opening of the spin gap. The same model can also be applied to fractional quantum Hall states via the composite fermion model. The composite fermion

Landau levels have exactly the same width as their electron counterparts, as previously suggested based upon a Dingle analysis of the low-field composite fermion oscillations [47]. The long tails of a Lorentzian are essential for the activation model, providing localized states deep in the gap, which are required to reproduce the robust high-temperature part of the $B_c(T)$ phase diagram. This is in agreement with published torque measurements, the detailed analysis of which concluded that Lorentzian broadening provided the best fits to the sawtoothlike oscillations in the 2DEG magnetization [5].

ACKNOWLEDGMENTS

This work was partially supported by ANR JCJC Project milliPICS, the Region Midi-Pyrénées under Contract No. MESR13053031, and IDEX Grant BLAPHENE.

[1] K. v. Klitzing, G. Dorda, and M. Pepper, Phys. Rev. Lett. **45**, 494 (1980).
[2] K. von Klitzing, Rev. Mod. Phys. **58**, 519 (1986).
[3] D. R. Leadley, R. J. Nicholas, J. J. Harris, and C. T. Foxon, Phys. Rev. B **58**, 13036 (1998).
[4] B. A. Piot, D. K. Maude, M. Henini, Z. R. Wasilewski, K. J. Friedland, R. Hey, K. H. Ploog, A. I. Toropov, R. Airey, and G. Hill, Phys. Rev. B **72**, 245325 (2005).
[5] A. Potts, R. Shepherd, W. G. Herrenden-Harker, M. Elliott, C. L. Jones, A. Usher, G. A. C. Jones, D. A. Ritchie, E. H. Linfield, and M. Grimshaw, J. Phys.: Condens. Matter **8**, 5189 (1996).
[6] M. Zhu, A. Usher, A. J. Matthews, A. Potts, M. Elliott, W. G. Herrenden-Harker, D. A. Ritchie, and M. Y. Simmons, Phys. Rev. B **67**, 155329 (2003).
[7] A. Usher and M. Elliott, J. Phys.: Condens. Matter **21**, 103202 (2009).
[8] D. C. Tsui, H. L. Stormer, and A. C. Gossard, Phys. Rev. Lett. **48**, 1559 (1982).
[9] R. B. Laughlin, Phys. Rev. Lett. **50**, 1395 (1983).
[10] R. Willett, J. P. Eisenstein, H. L. Störmer, D. C. Tsui, A. C. Gossard, and J. H. English, Phys. Rev. Lett. **59**, 1776 (1987).
[11] H. L. Stormer, D. C. Tsui, and A. C. Gossard, Rev. Mod. Phys. **71**, S298 (1999).
[12] H. L. Stormer, Rev. Mod. Phys. **71**, 875 (1999).
[13] J. K. Jain, Phys. Rev. Lett. **63**, 199 (1989).
[14] H. P. Wei, D. C. Tsui, M. A. Paalanen, and A. M. M. Pruisken, Phys. Rev. Lett. **61**, 1294 (1988).
[15] A. M. M. Pruisken, Phys. Rev. Lett. **61**, 1297 (1988).
[16] S. L. Sondhi, S. M. Girvin, J. P. Carini, and D. Shahar, Rev. Mod. Phys. **69**, 315 (1997).
[17] P. L. McEuen, A. Szafer, C. A. Richter, B. W. Alphenaar, J. K. Jain, A. D. Stone, R. G. Wheeler, and R. N. Sacks, Phys. Rev. Lett. **64**, 2062 (1990).
[18] S. Koch, R. J. Haug, K. v. Klitzing, and K. Ploog, Phys. Rev. Lett. **67**, 883 (1991).
[19] D.-H. Lee, Z. Wang, and S. Kivelson, Phys. Rev. Lett. **70**, 4130 (1993).
[20] P. T. Coleridge, Phys. Rev. Lett. **72**, 3917 (1994).
[21] D.-H. Lee, S. A. Kivelson, Z. Wang, and S.-C. Zhang, Phys. Rev. Lett. **72**, 3918 (1994).
[22] W. Pan, D. Shahar, D. C. Tsui, H. P. Wei, and M. Razeghi, Phys. Rev. B **55**, 15431 (1997).
[23] D. Shahar, D. C. Tsui, M. Shayegan, E. Shimshoni, and S. L. Sondhi, Phys. Rev. Lett. **79**, 479 (1997).
[24] D. Shahar, M. Hilke, C. Li, D. Tsui, S. Sondhi, J. Cunningham, and M. Razeghi, Solid State Commun. **107**, 19 (1998).
[25] P. T. Coleridge, Phys. Rev. B **60**, 4493 (1999).
[26] L. Ponomarenko, D. de Lang, A. de Visser, D. Maude, B. Zvonkov, R. Lunin, and A. Pruisken, Phys. E (Amsterdam, Neth.) **22**, 236 (2004).
[27] L. A. Ponomarenko, Ph.D. thesis, University of Amsterdam, 2005.
[28] D. T. N. de Lang, Ph.D. thesis, University of Amsterdam, 2005.
[29] A. de Visser, L. A. Ponomarenko, G. Galistu, D. T. N. de Lang, A. M. M. Pruisken, U. Zeitler, and D. Maude, J. Phys.: Conf. Ser. **51**, 379 (2006).
[30] D. T. N. de Lang, L. A. Ponomarenko, A. de Visser, and A. M. M. Pruisken, Phys. Rev. B **75**, 035313 (2007).
[31] L. B. Rigal, D. K. Maude, M. Potemski, J. C. Portal, L. Eaves, J. R. Wasilewski, G. Hill, and M. A. Pate, Phys. Rev. Lett. **82**, 1249 (1999).
[32] N. F. Mott, Philos. Mag. **19**, 835 (1969).
[33] A. L. Efros and B. I. Shklovskii, J. Phys. C **8**, L49 (1975).
[34] Y. Ono, J. Phys. Soc. Jpn. **51**, 237 (1982).
[35] A. Briggs, Y. Guldner, J. P. Vieren, M. Voos, J. P. Hirtz, and M. Razeghi, Phys. Rev. B **27**, 6549 (1983).
[36] D. G. Polyakov and B. I. Shklovskii, Phys. Rev. Lett. **70**, 3796 (1993).
[37] D. G. Polyakov and B. I. Shklovskii, Phys. Rev. B **48**, 11167 (1993).
[38] F. Hohls, U. Zeitler, and R. J. Haug, Phys. Rev. Lett. **88**, 036802 (2002).
[39] A. Tzalenchuk, S. Lara-Avila, A. Kalaboukhov, S. Paolillo, M. Syväjärvi, R. Yakimova, O. Kazakova, T. J. B. M. Janssen, V. Falko, and Kubatkin, Nat. Nanotechnol. **5**, 186 (2010).
[40] T. J. B. M. Janssen, A. Tzalenchuk, S. Lara-Avila, S. Kubatkin, and V. I. Fal'ko, Rep. Prog. Phys. **76**, 104501 (2013).
[41] T. J. B. M. Janssen, S. Rozhko, I. Antonov, A. Tzalenchuk, J. M. Williams, Z. Melhem, H. He, S. Lara-Avila, S. Kubatkin, and R. Yakimova, 2D Mater. **2**, 035015 (2015).
[42] A. Raymond, J. L. Robert, and C. Bernard, J. Phys. C **12**, 2289 (1979).
[43] C. Weisbuch and C. Hermann, Phys. Rev. B **15**, 816 (1977).
[44] T. Ando and Y. Uemura, J. Phys. Soc. Jpn. **37**, 1044 (1974).
[45] K.-J. Friedland, R. Hey, H. Kostial, R. Klann, and K. Ploog, Phys. Rev. Lett. **77**, 4616 (1996).
[46] C. Faugeras, D. K. Maude, G. Martinez, L. B. Rigal, C. Proust, K. J. Friedland, R. Hey, and K. H. Ploog, Phys. Rev. B **69**, 073405 (2004).
[47] D. R. Leadley, R. J. Nicholas, C. T. Foxon, and J. J. Harris, Phys. Rev. Lett. **72**, 1906 (1994).
[48] R. R. Du, H. L. Stormer, D. C. Tsui, A. S. Yeh, L. N. Pfeiffer, and K. W. West, Phys. Rev. Lett. **73**, 3274 (1994).
[49] L. Eaves and F. W. Sheard, Semicond. Sci. Technol. **1**, 346 (1986).